

## Abstract

The Corona Australis star forming region, shown in Figure 1 and located approximately 130pc away, is situated just below the Galactic Plane. Presented are results from five wavebands given by *Herschel's*\* [Pilbratt *et al.* 2010] Spectral and Photometric Imaging REceiver (SPIRE) [Griffin *et al.* 2010] and Photodetector Array Camera and Spectrometer (PACS) [Poglitsch *et al.* 2010]. Pixel by pixel SED fitting has allowed calculation of temperature and mass estimates for the cold dust component of the region. Temperature within the region shows a broadly flat distribution; similar to the Taurus region, but unlike the Ophiuchus region. We present here the first results from the Herschel Gould Belt Survey [André *et al.* 2010] for prestellar and starless cores located by the source extraction algorithm *Getsources* [Men'shchikov *et al.* 2012]. The region to be relatively quiescent compared to Aquila [Könyves *et al.* 2010].

## Physical characteristics

The *Herschel* data show clear morphology that appears to be the result of interaction with an external force. The cometary structure arises from an interaction with the Upper Centaurus Lupus (UCL) association HI shell [de Geus 1990] whereby the cloud has been blown in an approximate direction of west to east, with the top of the image being north. It can be observed that this interaction has resulted in a sharp 'edge' at the westernmost extent. The *Spitzer* [Werner *et al.* 2004] MIPS  $24\mu\text{m}$  [Rieke *et al.* 2004] data in Figure 1 show the intermediate or 'warm' dust component within the Coronet, with emission being particularly prominent within the locale of the R, T, S and VV CrA variable stars. To the east of the Coronet there are several clumps that appear almost periodic to the eye, that are fragments of the bulk of the cloud. *Spitzer* data also show the streamer in the far east as highlighted by Peterson *et al.* 2011.

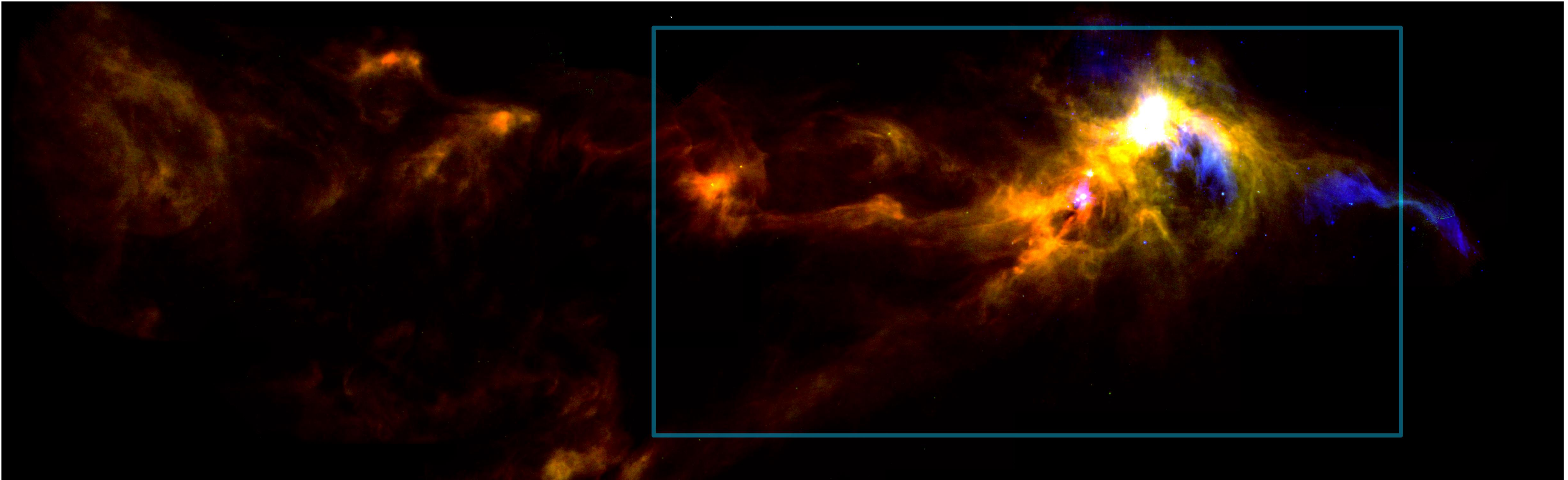


Figure 1: Three colour image of Corona Australis taken by Herschel SPIRE ( $250\mu\text{m}$ -red/orange) and PACS ( $160\mu\text{m}$ -green/yellow) and Spitzer MIPS ( $24\mu\text{m}$ -blue). The blue box contains the area designated as the western part of the cloud. It is this area for which this work is presented.

## SED fitting

The temperatures and masses of the region are well fitted by a greybody function of the form

$$F_\nu = \frac{B_\nu(T)M\kappa_\nu}{D^2},$$

where  $F_\nu$  is the flux density at a central frequency  $\nu$ ,  $\kappa_\nu$  is the dust mass opacity,  $M$  is the mass,  $B_\nu(T)$  is the Planck Function and  $D$  is the distance to the cloud. We consider the relation where  $\kappa_\nu \propto \nu^\beta$ , where  $\beta$  is the dust opacity exponent, which is fixed at  $\beta = 2$ . We are able to fit the greybody function utilising the MPFIT [Markwardt 2009] package, with which error maps are also produced. Column density is calculated as

$$N(H_2) = \frac{M}{m_H\mu A},$$

where  $N(H_2)$  is the column density,  $M$  is the mass in solar masses,  $m_H$  is the mass of a molecular hydrogen,  $\mu = 2.86$  is the mean molecular weight for hydrogen (see Kirk *et al.* 2013) and  $A$  is the area of a pixel. Producing the column density map allows mass estimation for sources within the cloud.

## Source extraction and filamentary structure

We proceed in running *Getsources* [Men'shchikov, 2012], a multi-wavelength, multi-scale extraction routine. We limit valid sources to those defined by having a high signal to noise, as well as splitting the starless and prestellar cores from the protostars using the presence of  $70\mu\text{m}$  emission from the PACS data following Könyves *et al.* (2010).

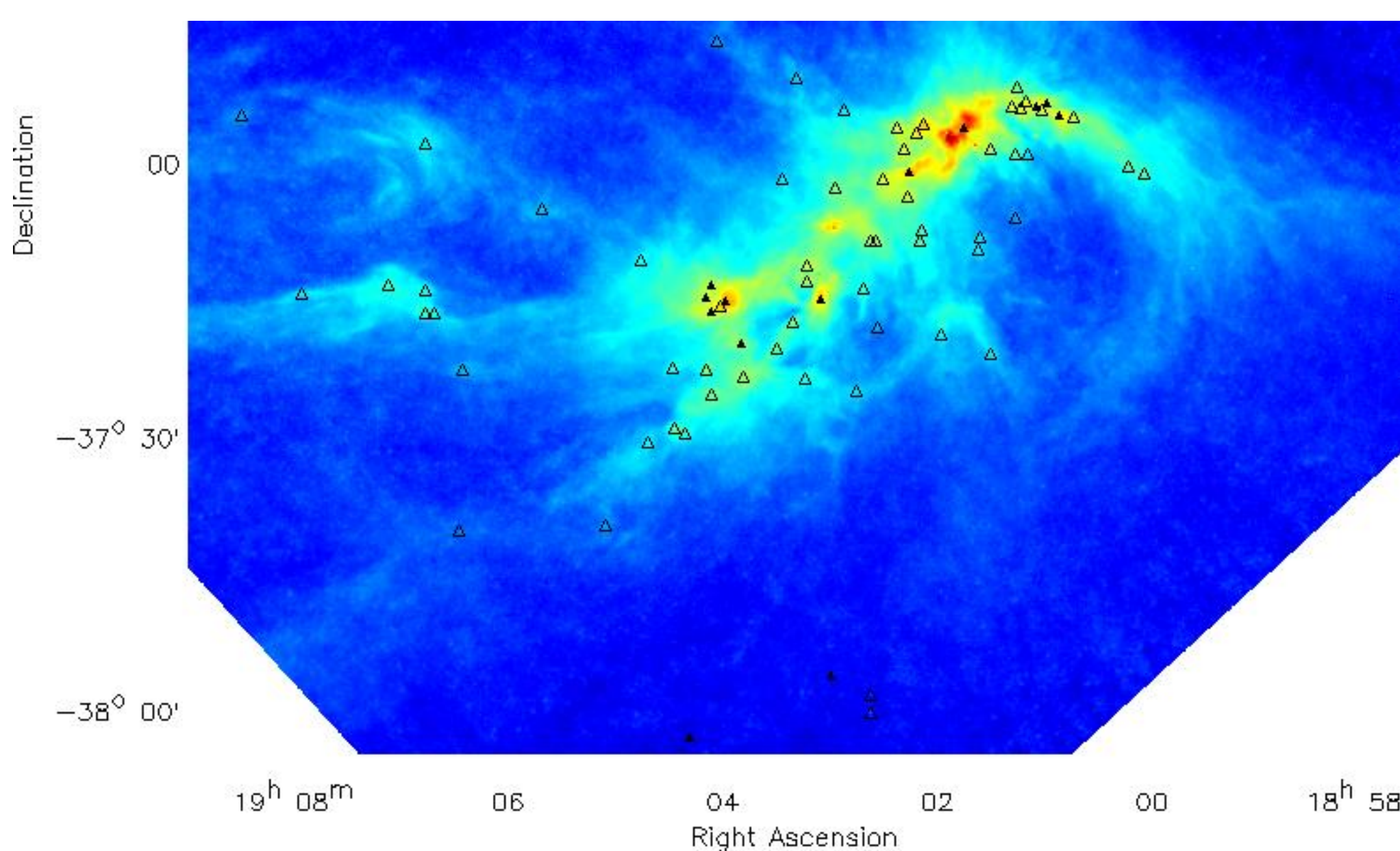


Figure 2: We overplot the locations of the sources that are located by *Getsources*. Filled black triangles are the locations of the prestellar cores, while hollow black triangles denote starless cores.

## Mass-size plot

Figure 2 shows the population of starless cores and prestellar cores as found by *Getsources*. We distinguish prestellar cores from starless cores as having a ratio  $\frac{M_{BE}}{M_c} < 2$ , where  $M_{BE}$  is the Bonnor-Ebert mass given by  $M_{BE} = 2.4 \frac{Rc^2}{G}$  [Bonnor, 1956] and  $M_c$  is the total mass of the source derived from the column density map.  $R$  is the deconvolved radius of the core and  $c$  is the isothermal sound speed given by  $c^2 = k_b T / \mu m_p$  where  $\mu = 2.86$  and  $m_p$  is the mass of a proton. The temperature  $T$  is derived from SED fitting to the source. We locate 11 prestellar cores and 64 starless cores (see Figure 3).

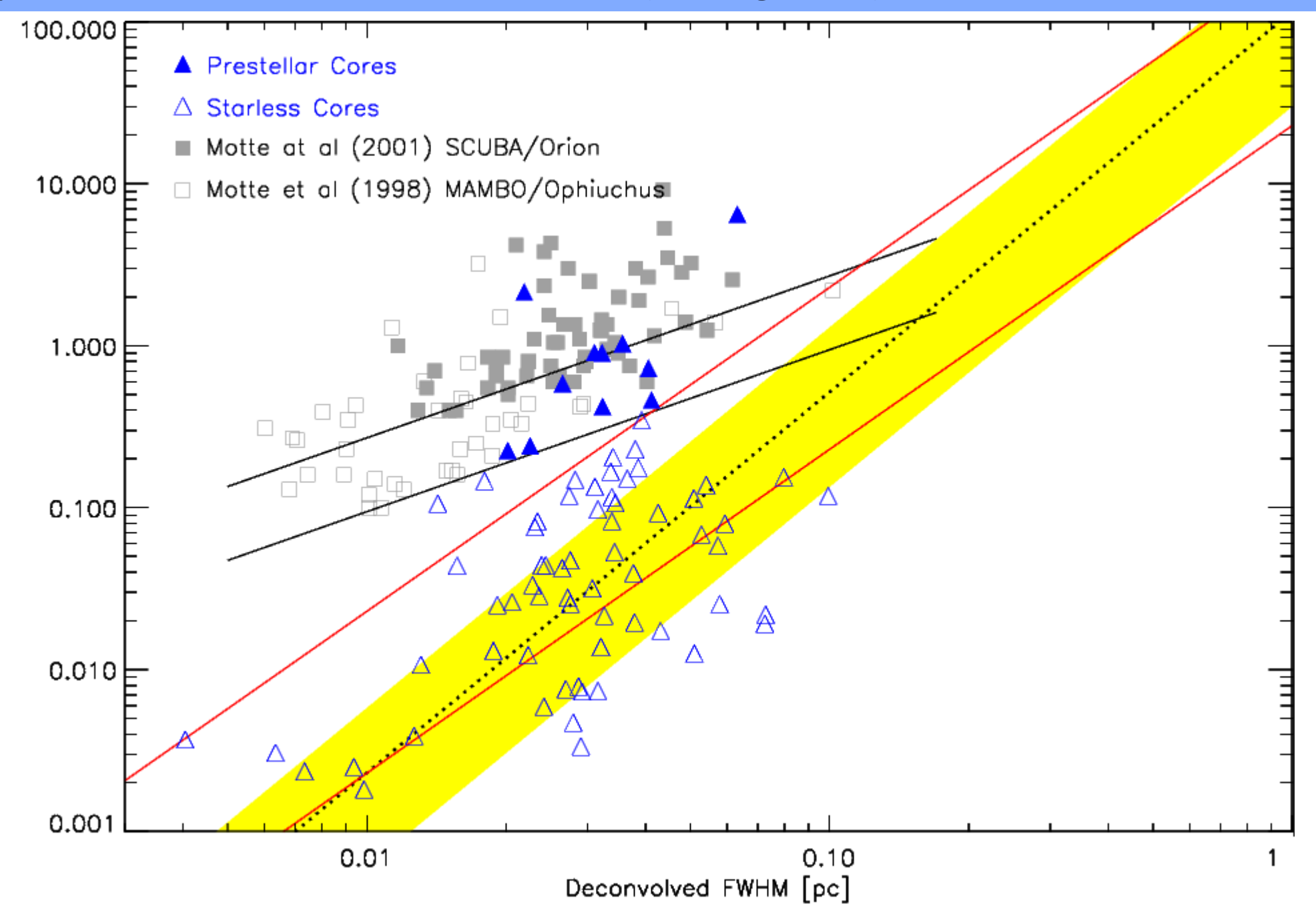


Figure 3: Mass size plot showing the distribution of starless and prestellar cores for the region in Figure 2. The two parallel red lines are the constant mean column densities at  $10^{21}\text{cm}^{-2}$  (lower) and  $10^{22}\text{cm}^{-2}$  (upper). The two black lines show the models of critical isothermal Bonnor-Ebert spheres for temperatures of  $T = 7\text{K}$  and  $T = 10.0\text{K}$ . The shaded yellow band shows the correlation for mass-size from Elmegreen and Falgarone (1996). Results for Motte *et al.* (2001, 1998) for SCUBA in the Orion region and MAMBO in the Ophiuchus region are overlaid for comparison. For similar plots see Kirk *et al.* (2013) and Könyves *et al.* (2010).

## References & Acknowledgement

- André, Ph., Men'shchikov, A., Bontemps, S., Könyves, V., Motte, F., Schneider, N., Didelon, P., *et al.* 2010. *A&A*, 518L, 102A.  
 Bonnor, W. D. 1956. *MNRAS*, 116, 351  
 de Geus, E. J. 1990. *A&A*, 262, 258.  
 Griffin, M. J., Abergel, A., Abreu, A., Ade, P. A. R., & André, Ph. *et al.* 2010. *A&A*, 518, L3.  
 Kirk, J. M., Ward-Thompson, D., Palmeirim, P., André, Ph. & Griffin, M. J. *et al.* 2013 *MNRAS*, 432, 1424.  
 Könyves, V., André, Ph., Men'shchikov, A., Schneider, N., Arzoumanian, D., Bontemps, S., Attard, M., Motte, F. *et al.* 2010. *A&A*, 518, L106  
 Markwardt, C. B. 2009. *Astronomical Data Analysis Software and Systems XVIII*, Quebec, Canada, ASP Conference Series, Vol. 411, eds. Men'shchikov, A., André, Ph., Didelon, P., Motte, F., Hennemann, M., Schneider, N. 2012. *A&A*, 542, A81.  
 Motte, F., André, Ph. & Neri R. 1998. *A&A*, 336, 150  
 Motte, F., André, Ph., Ward-Thompson, D. & Bontemps, S. 2001, 372, 41.  
 Peterson, D. E., Caratti o Garatti, Bourke, T. L. *et al.* 2011. *ApJS*, 194, 43P.  
 Pilbratt, G. L., *et al.* 2010 *A&A*, 518(July), L1.  
 Poglitsch, A., Waelkens, C., Geis, N., Feuchtgruber, H., Vandenbussche, B., Rodriguez, L., & Krause, O. *et al.* 2010. *A&A*, 518(July), L2.  
 Rieke, G., E. T. Young, C. W. Engelbracht, D. M. Kelly, F. J. Low, E. E. Haller. *et al.* 2004. *ApJS*, 154, 25  
 Werner, M., Roellig, T., Low, F., Rieke, G., Rieke, M., Hoffmann, W. *et al.* 2004. *ApJS*, 154, 1.  
 email : [dwbresnahan@uclan.ac.uk](mailto:dwbresnahan@uclan.ac.uk)  
 \**Herschel* is an ESA space observatory with science instruments provided by European-led Principal Investigator consortia and with important participation from NASA.